Remarkable Aliphatic Hydroxylation by the Diiron Enzyme Toluene 4-Monooxygenase in Reactions with Radical or Cation Diagnostic Probes Norcarane, 1,1-Dimethylcyclopropane, and 1,1-D...

ARTICLE *in* BIOCHEMISTRY · JANUARY 2005

Impact Factor: 3.02 · DOI: 10.1021/bi040033h · Source: PubMed

6 AUTHORS, INCLUDING:

Luke A Moe
University of Kentucky
37 PUBLICATIONS **408** CITATIONS
SEE PROFILE

David Deng
South China Normal University
19 PUBLICATIONS **263** CITATIONS
SEE PROFILE

Brian G Fox
University of Wisconsin–Madison
212 PUBLICATIONS **7,293** CITATIONS
SEE PROFILE

Remarkable Aliphatic Hydroxylation by the Diiron Enzyme Toluene 4-Monooxygenase in Reactions with Radical or Cation Diagnostic Probes Norcarane, 1,1-Dimethylcyclopropane, and 1,1-Diethylcyclopropane†

Luke A. Moe,‡ Zhengbo Hu,⊥ Dayi Deng,⊥ Rachel N. Austin,§ John T. Groves,⊥ and Brian G. Fox*,‡

Department of Biochemistry, College of Agricultural and Life Sciences, University of Wisconsin, Madison, Wisconsin 53706-1544, Department of Chemistry, Bates College, 5 Andrews Road, Lewiston, Maine 04240, and Department of Chemistry, Princeton University, Princeton, New Jersey 08544

Received July 1, 2004

ABSTRACT: Toluene 4-monooxygenase (T4MO) catalyzes the hydroxylation of toluene to yield 96% *p*-cresol. This diiron enzyme complex was used to oxidize norcarane (bicyclo[4.1.0]heptane), 1,1-dimethylcyclopropane, and 1,1-diethylcyclopropane, substrate analogues that can undergo diagnostic reactions upon the production of transient radical or cationic intermediates. Norcarane closely matches the shape and volume of the natural substrate toluene. Reaction of isoforms of the hydroxylase component of T4MO (T4moH) with different regiospecificities for toluene hydroxylation ($k_{cat} \approx 1.9-2.3$ s^{-1} and coupling efficiency ≈ 81−96%) revealed similar catalytic parameters for norcarane oxidation ($k_{cat} \approx 0.3-0.5$ s^{-1} and coupling efficiency ≈ 72%). The products included variable amounts of the un-rearranged isomeric norcaranols and cyclohex-2-enyl methanol, a product attributed to rearrangement of a radical oxidation intermediate. A ring-expansion product derived from the norcaranyl C-2 cation, cyclohept-3-enol, was not produced by either the natural enzyme or any of the T4moH isoforms tested. Comparative studies of 1,1-dimethylcyclopropane and 1,1-diethylcyclopropane, diagnostic substrates with differences in size and with ∼50-fold slower k_{cat} values, gave products consistent with both radical rearrangement and cation ring expansion. Examination of the isotopic enrichment of the incorporated O-atoms for all products revealed high-fidelity incorporation of an O-atom from O_2 in the un-rearranged and radical-rearranged products, while the O-atom found in the cation ring-expansion products was predominantly obtained by reaction with H_2O. The results show a divergence of radical and cation pathways for T4moH-mediated hydroxylation that can be dissected by diagnostic substrate probe rearrangements and by changes in the source of oxygen used for substrate oxygenation.

Biological hydrocarbon oxidation reactions are of paramount importance in maintaining the global carbon cycle (*1*−*5*), providing energy and carbon for cellular growth (*6*), and promoting the detoxification of drugs and other xenobiotics (*7*). Our understanding of biological strategies for substrate hydroxylation have emerged from studies of P450s (*8*−*10*), diiron enzymes such as methane monooxygenase [MMO,[1] (*11*−*13*)], other non-heme iron systems (*14*−*16*), and copper-containing particulate methane monooxygenase (*17*−*23*). Although these biocatalysts differ in cofactor content and in details of the generation and stabilization of the required oxidizing species, similar themes involving the participation of high-valent metal-oxo intermediates and the reactivity of various spin-state manifolds have emerged (*24*). Several fundamentally different, plausible mechanisms for the hydroxylation of aliphatic hydrocarbons are most-often considered for these reactions and are summarized in Figure 1. Figure 1A shows H-atom abstraction followed by either recombination of the substrate radical and oxidant ("rebound" mechanism (*9*, *25*)) or $2e^-$ oxidation to a cationic intermediate followed by recombination with solvent to yield ROH. Figure 1B shows that insertion of an O-atom into the C−H bond may also generate the product ROH. Alternatively, Figure 1C shows that the insertion of ^+OH can generate an $R-{}^+OH_2$ intermediate that may release either a proton to yield product ROH or H_2O (a "solvolysis" reaction) to yield a cationic intermediate capable of reacting with solvent to again yield product ROH.

Owing to high reactivity, the direct detection of radical and cationic intermediates is generally not feasible during hydrocarbon hydroxylation reactions. Thus a variety of experimental approaches have been used to assess the

† This work was supported by the National Science Foundation (Grants MCB-9733734 and MCB-0316232 to B.G.F., CHE-0116232 and CHE-0221978 to R.N.A., and CHE-0221978 and CHE-0316301 to J.T.G.) and the National Institutes of Health (Grant GM 036298 to J.T.G.).

* To whom correspondence should be addressed. Mailing address: 141B Biochemistry Addition, Department of Biochemistry, 433 Babcock Dr., University of Wisconsin, Madison, WI 53706. Phone: (608) 262−9708. Fax: (608) 262-3453. E-mail: bgfox@biochem.wisc.edu.

‡ University of Wisconsin.

§ Bates College.

⊥ Princeton University.

[1] T4MO, four-protein toluene 4-monooxygenase complex from *Pseudomonas mendocina* KR1; T4moH, hydroxylase component of T4MO; MMO, methane monooxygenase; MMO OB3b, MMO from *Methylosinus trichosporium* OB3b; MMO (Bath), MMO from *Methylococcus capsulatus* (Bath); P450, cytochrome P450 monooxygenase; 1,1-DMCP, 1,1-dimethycyclopropane; 1,1-DECP, 1,1-diethylcyclopropane.

10.1021/bi040033h CCC: $27.50
Published on Web 11/20/2004

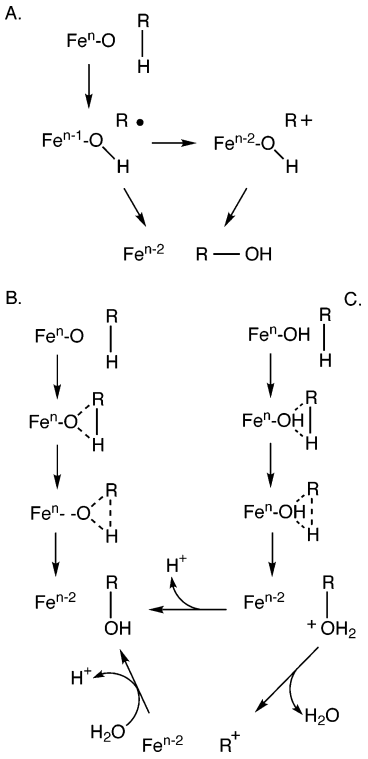

FIGURE 1: Plausible pathways of hydrocarbon hydroxylation: (A) radical "rebound" or $2e^-$ oxidation and recombination of R^+ with metal-bound water; (B) insertion of [O] into the C−H bond to yield R−OH; (C) insertion of [$^+$OH] followed by either release of H^+ to yield R−OH or release of H_2O ("solvolysis") to yield R^+, which then reacts with water.

mechanisms and potential contributions of the pathways indicated in Figure 1. Some of these approaches include measurement of steady- and transient-state kinetic isotope effects (*26*, *27*), determination of the epimerization of stereospecifically labeled substrates (*28*−*30*), computational approaches (*31*−*35*), and reaction of substrate analogues that give rise to rearrangement products diagnostic for different oxidation pathways (*36*−*41*). When undertaken with diagnostic substrate analogues the rearrangement rates of which have been measured, this approach has been called the "radical-clock" method (*42*, *43*). One prominent application of the radical-clock method has been to estimate the lifetime of radical intermediates in both enzymatic and nonenzymatic hydroxylations (*9*, *10*), while a related approach has been to evaluate analogues that give unique products diagnostic for both radical- and cation-based oxidation manifolds. Recent experiments have included the synthesis of new analogues with increasingly fast rearrangement rates (*44*−*46*). In general, enhancement of the gas-phase reactivity has required introduction of additional functional groups that impart molecular volumes and shapes of both substrates and products not necessarily compatible with the binding pocket present in a natural enzyme active site. Consequently, these analogues have structures that differ considerably from the physiologically relevant substrates, which can lead to low turnover rates, inefficient coupling of electron transfer, low product yields, and other characteristic indicators of altered enzyme performance. Associated with these results, the potential contributions of the enzyme active site to the stability of substrate intermediates and their potential rearrangement reactions must also be considered.

Toluene 4-monooxygenase (T4MO) is a soluble, multicomponent diiron enzyme that catalyzes the NADH- and O_2-dependent, high-regiospecificity oxidation of toluene to *p*-cresol (*47*). For this enzyme, the high fidelity of reaction with toluene has apparently evolved from mechanistic demands introduced by the subsequent enzymatic steps in the metabolic pathway of *Pseudomonas mendocina* KR1 (*48*). T4MO can also catalyze the oxidation of a wide variety of non-native substrates with size similar to toluene including alkanes, alkenes and aromatic and heteroaromatic compounds (*49*−*51*), and many of these reactions also exhibit high selectivity for the position of oxidation. Moreover, T4moH isoforms with comparable kinetic properties but with distinct patterns of regiospecificity for the hydroxylation of toluene and other substrates have been produced and characterized (*52*).

In this work, the reactivity of T4moH and three well-characterized isoforms (T201A, T201S, and G103L) has been examined. The k_{cat} and k_{cat}/K_M values of these isoforms differ by only ∼20% for toluene oxidation, while the coupling efficiencies are 80% or higher (*52*). However, these isoforms also exhibit markedly different patterns of regiospecificity during the oxidation of toluene, the natural T4moH isoform yielding ∼96% *p*-cresol and the G103L isoform yielding a mixture of 55% *o*-cresol, 24% *m*-cresol, and 20% *p*-cresol. The overall similarity in catalytic properties associated with the distinct regiospecificities provides a unique basis for this study of the reactions of "radical-clock" substrates within closely related active sites.

Norcarane is a simple aliphatic substrate analogue that has been used to distinguish between cationic and radical oxidation pathways (*53*). Norcarane has a shape and size that closely matches that of toluene. The stereo overlay of toluene and norcarane shown in Figure 2, top panel, reveals the close structural similarity of these compounds. The six ring carbons of these two molecules overlay with an rms deviation of 0.272 Å^2, and the methyl group and cyclopropyl ring can also be roughly aligned to approximate a potential binding orientation in the enzyme active site. Moreover, these two molecules have similar solvent-exposed surface areas (399 Å^2 for toluene and 471 Å^2 for norcarane).

We have proposed that the high regiospecificity of the T4moH reaction with monosubstituted benzenes [e.g., toluene, nitrobenzene, chlorobenzene, and methoxybenzene (*51*, *52*, *54*)] involves a well-defined binding interaction between the substrate and enzyme active site. Furthermore, upon the basis of intramolecular isotope effect studies and deuterium shift patterns, a transient formation of a 3,4-arene oxide that undergoes directed opening toward 4-hydroxylation by interactions with the metal center has been proposed to account for the regiospecificity (*55*). In Figure 2, top panel, the C-3 and C-4 positions of toluene, indicated as small green spheres, nearly superimpose with the aligned C-2 and C-3 positions of norcarane. The mechanistically relevant 2-*endo*- and 2-*exo*-hydrogens of norcarane are indicated as small white spheres. These hydrogen atoms lie ∼2.4 and ∼3.5 Å from the bridgehead carbon position, respectively.

Norcarane has proven to be an excellent substrate for all T4MO isoforms tested, leading to a clearer understanding of catalysis with respect to a radical-clock analogue. Comparative studies of 1,1-dimethylcyclopropane and 1,1-diethylcyclopropane, two additional diagnostic substrate analogues

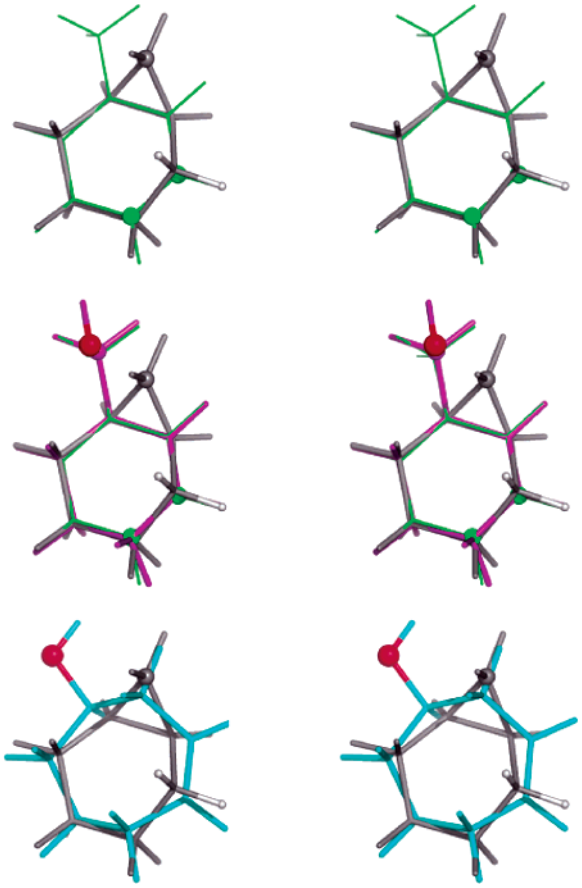

FIGURE 2: Stereo representations of the substrates and products under investigation. The ring carbon atoms of norcarane and toluene were aligned and oriented to place the cyclopropane ring of norcarane adjacent to the methyl group of toluene. The top panel shows norcarane (gray) and toluene (green). The middle panel shows norcarane (gray), cyclohex-2-enyl methanol (purple), and toluene (green). The bottom panel shows norcarane (gray) and cyclohept-3-enol (cyan). Positions of oxygen atoms are shown in red.

with ~50-fold slower k_{cat} values than either toluene or norcarane, were also undertaken. The combined results indicate that the nature of both the substrate and the T4moH active site influences the reactivity of intermediates leading to diagnostic product distributions. Un-rearranged, radical-rearranged, and cation ring-expansion products were identified and further characterized by isotopic labeling in the presence of $^{18}O_2$ and $^{18}OH_2$ during oxidation reactions. Results with all three substrate analogues revealed that both the un-rearranged alcohol and the radical-rearranged products had a high percentage of O-atom incorporation (>80−95%) from $^{18}O_2$, while the cation products had O-atom incorporation largely derived from solvent. Possibilities accounting for the differences in product distributions and isotopic incorporation are discussed.

MATERIALS AND METHODS

Chemicals. Chloroform (99+% HPLC grade), toluene, isomeric cresols, β-NADH, Sil-A derivatizing reagent, 3-methylbenzyl alcohol, and decane (99+%) were from Sigma-Aldrich (St. Louis, MO) and used without further purification. The synthesis of norcarane and norcarane products, methods used for GC/MS separations, and analysis of the mass spectral fragmentation patterns obtained from these compounds were described elsewhere (*41*). 1,1-DMCP was obtained from Pfaltz & Bauer (Waterbury, CT), and additional 1-methylcyclopropane methanol, 3-methyl-3-buten-1-ol, 3-methyl-2-buten-1-ol, 2-methyl-3-buten-1-ol, 2-methyl-3-buten-2-ol, and 1-methylcyclobutanol were from Sigma-Aldrich. These compounds were used without further purification. 1,1-DECP (99%) was purchased from Chemsampco, Inc. (Trenton, NJ). 1-Ethyl-2-methylcyclobutanol was synthesized by addition of CH_3CH_2MgBr to 2-methylcyclobutanone, which were made according to the literature (*56*). 3-Ethyl-3-penten-1-ol was synthesized according to the literature (*57*). 1-Ethylcyclopropylethanol was synthesized from 2-ethyl-3-hydroxy-1-butene by use of the Simmons−Smith reaction (*58*). Isotopically enriched $^{18}O_2$ (99% as originally purchased) and $^{18}OH_2$ (95%) were from ICON (Summit, NJ).

Molecular Modeling. Structures of substrates and products were energy-minimized using Gaussian 98 (Wallingford, CT). Substrate and product structures were aligned, and rms deviations and atomic distances were calculated using the pair_fit routine of MacPyMOL (version 0.95, DeLano Scientific LLC, Castro City, CA). Solvent-exposed surface areas were calculated using a probe sphere with a 1.4 Å radius and the get_area routine of MacPyMOL.

T4MO Components. The T4moH isoforms were created by overlap extension PCR using pRS204 as the template for the T201A and T201S isoforms (*54*) and pKM10 as the template for the G103L isoform (*52*). All T4MO components were independently expressed in *Escherichia coli* BL21 (DE3) (Novagen, Madison, WI), purified, and characterized according to published procedures (*59*−*61*).

Enzyme Reactions. A typical reaction was performed at 26 °C in 50 mM phosphate buffer, pH 7.5, containing 1 nmol of T4moF reductase, 10 nmol of T4moC Rieske ferredoxin, 10 nmol of T4moD effector protein, and 5 nmol of T4moH (based on $\alpha\beta\gamma$ protomer, corresponding to active site concentration). The reaction vial was sealed with a crimp-top Teflon septum, and neat substrate (typically 1−3 μL) was added to the reaction mixture by injection onto the sidewall of the reaction vial using a gastight syringe. The mixture was allowed to incubate for 1−2 min prior to initiation of the reaction by the addition of NADH to an initial concentration of ~25 mM and a final volume of 250 μL. The reaction was continued for the specified time (up to 3 min for kinetic assays; 7 min for product accumulation studies) and then quenched by extraction into an equal volume of neat $CHCl_3$ for routine assays, and either $CHCl_3$/decane (25 μM) for kinetic assays with norcarane or $CHCl_3$/3-methylbenzyl alcohol (50 μM) for kinetic assays with 1,1-DMCP. Decane and 3-methybenzyl alcohol were added as internal standards for GC analysis. The quenched solution was vortexed for 30 s and centrifuged for 2 min at 14 000 rpm. The organic layer was removed and immediately analyzed by either GC/MS using an HP-5MS 5% phenylmethyl siloxane column or GC/FID using a SGE BP20 Carbowax column. Separation conditions and analytical methods for the norcarane oxidation products have been previously reported (*10*, *14*, *41*). For 1,1-DMCP and products, the following temperature program was used with the SGE BP20 column: 50 °C for 5 min; 50−240 °C at 10 °C/min; 240 °C for 10 min. Product analyses for 1,1-DECP were as previously reported (*10*). Control reactions containing

enzyme components were treated identically to other assays with the exception that NADH was not added.

The k_{cat} values were determined as previously described (*52*) with saturated solutions of substrate and calculated based on similarly extracted and analyzed authentic products of known concentration. For norcarane, the total products derived from oxidation at the C-2 position were separated into un-rearranged and rearranged fractions, and the ratio of these two was used to estimate radical lifetime based on the rearrangement rate of 2×10^8 s^{-1} (*15*).

Coupling Efficiency Determinations. Coupling efficiency is defined as the ratio of nanomoles of product produced relative to nanomoles of NADH consumed. A Hewlett-Packard 8452A diode array spectrophotometer equipped with magnetic stirring and temperature control was used for these meaurements. All reactions were performed at 26 °C in a septum-sealed optical cuvette in a total reaction volume of 1 mL of norcarane-saturated 50 mM phosphate buffer, pH 7.5, containing 1 nmol of T4moF reductase, 10 nmol of T4moC Rieske ferredoxin, 10 nmol of T4moD effector protein, 5 nmol of T4moH (based on $\alpha\beta\gamma$ protomer), and ~600 nmol of NADH. The concentration of the NADH stock solution was determined using $\epsilon_{340} = 6220$ M^{-1} cm^{-1}. To initiate the reaction, an aliquot of the NADH stock solution was added to the reaction mixture, the cuvette was capped, and the absorbance change was monitored at 340 nm until no further change was observed (typically ~15−20 min). After this time, the reaction was extracted as described above and analyzed by GC/MS to obtain the concentration of products.

Studies Using $^{18}O_2$. These reactions were assembled in an O_2-free glovebox chamber (Coy Laboratory Products Inc., Grass City, MI) containing ~2−3% H_2 in a N_2 atmosphere. All syringes, reaction vials, septa, and other materials required for the $^{18}O_2$ experiments were stored in the glovebox chamber. Samples of 50 mM phosphate buffer, pH 7.5, were sparged with O_2-free Ar gas and then transferred into the glovebox chamber. For studies of norcarane reactions, frozen aliquots of NADH and each of the four T4MO components were removed from storage in a −80 °C freezer and cycled into the glovebox chamber by repeated flushing and filling of the ante-chamber with N_2 before the samples were thawed. Once inside the glovebox chamber, 2 nmol of T4moF reductase, 20 nmol of T4moC Rieske ferredoxin, 20 nmol of T4moD effector protein, and 10 nmol of T4moH (based on $\alpha\beta\gamma$ protomer) were added to a Wheaton vial (8 μL total volume), followed by the addition of the anaerobic phosphate buffer solution. The vial was sealed with a rubber septum and further sealed with electrical tape. The NADH was transferred to a glass insert placed in a screw cap conical vial and sealed with a silcone/Teflon septum. A 2 mL gastight and stopper-sealable syringe was filled to 2 mL with the atmosphere of the glovebox chamber and sealed. The protein mixture, NADH, and 2 mL syringe were then removed from the glovebox chamber. The contents of the 2 mL syringe were exchanged with 2 mL of $^{18}O_2$ gas from a gas bulb and immediately injected into the reaction vial containing the protein mixture. Norcarane (1−3 μL) was added to the sidewall of the reaction vial, and the mixture was allowed to shake at 26 °C for 1−2 min before the addition of the anaerobic NADH solution (15 μL, initial concentration of ~25 mM in the reaction vial). The final volume of enzyme reaction was 250 μL. After 7 min, the entire reaction mixture was quenched by the addition of 250 μL of neat $CHCl_3$ into the reaction vial. The reaction mixture was vortexed for 1 min and separated by centrifugation for 3 min at 14 000 rpm. The organic layer was extracted and analyzed by GC/MS as described above.

A separate experiment using $^{18}O_2$ with a lower unknown isotopic enrichment was also performed as described above and allowed to react for 7 min. After 7 min, 1 μL of toluene was added, and the reaction was allowed to continue for 1.5 min. This reaction mixture was separated and analyzed as described above. The isotopic enrichment in *p*-cresol was subsequently determined to be 65%, providing a calibration of the $^{18}O_2$ content in the gas of the reaction vial.

For 1,1-DMCP, and 1,1-DECP, the enzyme reactions were performed as above, except that the enzyme mixture and the NADH were first made anaerobic on a vacuum manifold through repeated cycles of flushing and filling with Ar. The protein and the NADH were then cycled into the glovebox chamber, and subsequent steps were completed as described above with the exception that toluene was not added during these reactions.

Studies Using $^{18}OH_2$. For these experiments, 1 nmol of T4moF reductase, 10 nmol of T4moC Rieske ferredoxin, 10 nmol of T4moD effector protein, and 5 nmol of T4moH were added to a Wheaton reaction vial. The enzyme components contributed 10 μL to the total reaction volume of 250 μL. A concentrated phosphate buffer (12 μL of 1 M solution, pH 7.5) was added to the protein components, and then either natural abundance or ^{18}O-enriched water (95%) was added to give an intermediate volume of either 242 μL for the substrate analogue reactions or 244 μL for toluene reactions. The reaction vial was capped and substrate (3 μL of the substrate analogue or 1 μL of toluene) was added using a gastight syringe. The enzyme reaction was initiated in the sealed reaction vial by addition of 5 μL of a concentrated NADH solution to give an initial concentration of ~10 mM using a gastight syringe. The reaction was allowed to proceed at 26 °C for 5 min, and the mixture was extracted and further analyzed as described in Studies Using $^{18}O_2$. After the dilution by the various reaction constituents was accounted for, these reaction vials contained ~85% enrichment of ^{18}O in water.

Analysis of ^{18}O Content in Reaction Products. The percentage of product containing an ^{18}O atom was determined from the integrated peak intensities of characteristic MS fragments for each product known to contain an O-atom. Where required, baseline corrections were made by comparison with reaction control samples. For norcarane, the characteristic MS fragments were $m/z = 111$ and 113 for 2-norcaranol and $m/z = 112$ and 114 for cyclohex-2-enyl methanol. For 1,1-DMCP, the organic extract was derivatized with Sil-A (Sigma), and the trimethylsilyl ethers were resolved by GC/MS. The ^{18}O incorporation percentages were based on evaluation of the following MS fragments: $m/z =$ 115 and 117, 130 and 132, and 143 and 145. For 1,1-DECP products, the characteristic MS fragments were $m/z = 86$ and 88 for the un-rearranged alcohol, $m/z = 114$ and 116 for the radical-rearranged alcohols, and $m/z = 57$ and 59 for the cyclobutanols.

Reaction Workup Controls. Solvolysis results for norcaranols are reported elsewhere (*10*). These additional procedures

were performed to investigate the potential contribution of reaction workup conditions to the observed product distributions.

To investigate the potential for nonenzymatic production of 1-methylcyclobutanol during enzyme reactions with 1,1-DMCP, aqueous 1-methylcyclopropanemethanol was extracted with several different commercial preparations of $CHCl_3$ to determine whether trace contamination with HCl could lead to the formation of 1-methylcyclobutanol via acid-catalyzed rearrangement. As an additional control, 50 μL of the aqueous 1-methylcyclopropanemethanol was added to 50 μL of 1 M HCl and incubated at room temperature for ~3 min before extraction with $CHCl_3$. These samples were analyzed by GC/MS and no 1-methylcyclobutanol was detected. 1-Methylcyclopropanemethanol was also incubated with T4MO under both turnover and nonturnover conditions, and the mixtures were subjected to the reaction workup described above for 1,1-DMCP assays. Again, no 1-methylcyclobutanol was detected. For comparison, acid-catalyzed isomerization of 1-methylcyclopropanemethanol in $^{18}OH_2$ with 1 M HCl at 100 °C for 60 min resulted in ~100% incorporation of the ^{18}O atom into 1-methylcyclobutanol (*62*). As an additional control, secondary oxidation of the un-rearranged 1-methylcyclopropanemethanol was not obtained during the 3−7 min time period of the typical T4moH reactions.

For control studies with 1,1-DECP, 100 μL of an enzyme reaction mixture containing 1,1-DECP was quenched with an equal volume of $CHCl_3$ after 7 min. The remaining reaction mixture was allowed to continue for an additional 20 min, after which 100 μL of the aged reaction was quenched with an equal volume of $CHCl_3$. Both extracts were analyzed by GC/MS, and the ratios of the un-rearranged, radical-rearranged, and cation ring-expansion products in these two samples were identical, indicating that there was no time-dependent conversion of the un-rearranged species to the cation ring-expansion product during the enzyme reaction or the sample workup.

From another standard 1,1-DECP reaction, 100 μL was quenched into an equal volume of 1 M HCl, and the quenched mixture was allowed to incubate for 5 min. The quenched mixture was then extracted with $CHCl_3$. The GC/MS analysis of this extract showed a decrease in the un-rearranged 1-(1-ethylcyclopropyl)-ethanol and a comparable increase in 1-methyl-2-ethylcyclobutanol (cation ring-expansion product). Furthermore, the triflates of either 1-ethylcyclopropylethanol or 1-ethyl-2-methylcyclobutanol were solvolyzed in 30% acetone−water and 80% acetone−water solutions. These solutions were kept in a capped reaction vial with a small amount of $CaCO_3$ at the bottom to neutralize the acid produced and incubated at 75 °C for 24 h. The products were isolated by extraction with CH_2Cl_2 and analyzed by GC-MS as described above. In these separate reactions, both 1-ethylcyclopropylethanol and 1-ethyl-2-methylcyclobutanol were recovered with a product distribution in the range of 1:1 to 2:1, respectively.

RESULTS

Kinetic Measurements. Table 1 contains a comparison of the k_{cat} values and coupling efficiencies obtained from the oxidations of norcarane and toluene by T4MO. These results show that the k_{cat} values for norcarane (~0.4−0.5 s^{-1}) differed from those obtained with toluene (~1.9−2.3 s^{-1}) by only 4- to 6-fold. Moreover, the coupling efficiency determined for reaction with norcarane (~72%) was only moderately lower than that observed for toluene (~95%). For comparison, T4moH gave k_{cat} = 0.2 s^{-1} and 65% coupling during the oxidation of nitrobenzene and k_{cat} = 0.13 s^{-1} and ~3% coupling with cyclohexane (*52*), reinforcing the overall correlation between k_{cat} and coupling. By this characterization, norcarane is a remarkably good substrate for T4MO, an enzyme that has been evolutionarily specialized for reaction with toluene. Since norcarane and toluene have overall similar shapes and volumes (Figure 2, top panel), we hypothesized that the catalytic ability of T4MO with norcarane may have arisen in part from this similarity. Thus the ability of norcarane to undergo characteristic rearrangement reactions within an apparently well-matched active site was of particular interest.

Table 1: Comparison of k_{cat} Values and Coupling in Toluene 4-Monooxygenase Reactions with Toluene and Norcarane

	toluene		norcarane	
T4MO isoform[a]	k_{cat} (s^{-1})[b]	coupling (%)[b]	k_{cat} (s^{-1})	coupling (%)
T4moH	2.3	94 ± 8	0.49 ± 0.04	72 ± 17
T201A	2.3	90	0.40 ± 0.03	*c*
T201S	1.9	88	0.35 ± 0.03	*c*
G103L	1.9	81	0.46 ± 0.02	*c*

[a] Natural T4moH and isoforms produced by mutagenesis as described in Materials and Methods. [b] k_{cat} values determined in the presence of saturating substrate, NADH, and O_2 and optimized concentration of the protein components of the T4MO complex. Coupling is defined as the ratio (expressed as a percentage) of the total hydroxylated products obtained relative to total NADH consumed as determined in reactions described in Materials and Methods. k_{cat} values and coupling for toluene were from ref *52*. The K_m values could not be measured with a suitable degree of accuracy due to the relatively low solubility of norcarane. [c] Not determined.

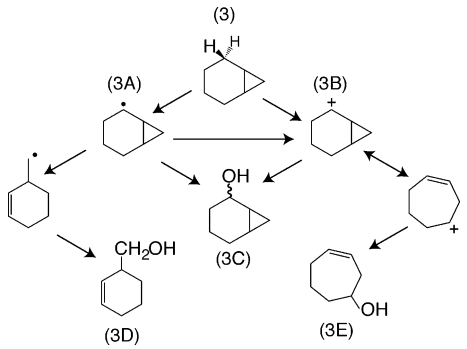

FIGURE 3: Reaction pathways of norcarane derived from either radical or cationic intermediates during oxidation at the C-2 position.

Analysis of Norcarane Reaction Products. Figure 3 shows reaction pathways involving initial oxidation at the mechanistically relevant C-2 position of norcarane (hydroxylation at the C-3 position does not provide additional mechanistic information). The radical oxidation manifold originates with a 2-norcaranyl radical (**3A**), while the cation oxidation manifold can arise from several different processes. The potential products are the isomeric *endo*-2- and *exo*-2-norcaranols (**3C**), cyclohex-2-enyl methanol (**3D**), and cyclohept-3-enol (**3E**).

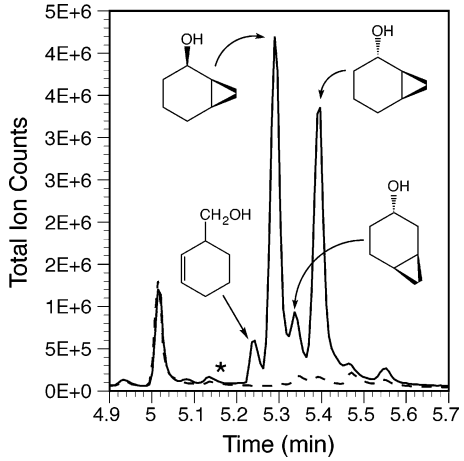

FIGURE 4: Representative GC elution profile of products obtained from T4MO-catalyzed reaction with norcarane (solid line). The dotted line shows the elution profile obtained from a control reaction containing all constituents indicated in Materials and Methods except NADH. The peak at ~5 min is decane added as an internal standard. The asterisk indicates the elution time of 5.17 min observed for authentic cyclohept-3-enol.

Figure 4 shows a representative GC elution profile of the products obtained during the reaction of T4moH with norcarane (solid line) and a baseline control reaction (dotted line). Control experiments with synthetic standards confirmed the baseline separation of cyclohept-3-enol, cyclohex-2-enylmethanol, *exo*-3-norcaranol, and *endo*-2-norcaranol, while additional studies showed that the *exo*-2- and *endo*-3-norcaranols coeluted at 5.4 min. The presence of the individual isomers within the 5.4 min peak could be estimated by differences in the parent region of the mass spectrum (m/z = 111 and 112).

endo-2-Norcaranol (Figure 4) accounted for ~48% of the total product distribution. Furthermore, examination of the fragmentation pattern within the 5.4 min peak suggested that the predominant product was *exo*-2-norcaranol, accounting for another ~39% of total products. Thus oxidation at the C-2 position of norcarane was clearly favored in T4moH reactions (Table 2). *exo*-3-Norcaranol was also observed as a lesser product (~9%). The C-2 and C-3 norcaranones have been identified as products in other studies of norcarane reactivity, possibly arising from secondary oxidations of the corresponding alcohols during the extended time period required for the enzyme reactions. The small GC peak observed with retention times of ~5.5 min may represent a negligible amounts of 3-ketone product formed in the short time period of the T4MO reactions (3−7 min).

During the T4moH-catalyzed oxidation studies, cyclohex-2-enyl methanol (**3D)** was reproducibly obtained as 4.5% ± 0.9% of the total products (Figure 4 and Table 2). In contrast, no cyclohept-3-enol (**3E)** was observed at the limit of detect of ~0.1% of total products. The asterisk symbol in Figure 4 indicates the elution time determined from an authentic sample of chemically synthesized cyclohept-3-enol. Analysis of the mass spectrum confirmed that the peak eluting just before this elution time was not cyclohept-3-enol.

Oxidation Results with T4moH Isoforms. Table 1 shows the catalytic parameters and Table 2 shows the product distributions obtained from norcarane for each of the T4moH isoforms tested. Owing to the similar catalytic parameters (Table 1), similar amounts of total products were obtained from each isoform. In distinction to the result with the natural T4moH, *exo*-2-norcaranol represented the majority product with each of the T4moH isoforms. Furthermore, the T4moH isoforms gave statistically significant differences in the amounts of the rearrangement product cyclohex-2-enyl methanol. Thus the T201A isoform gave a 30% higher fraction of cyclohex-2-enyl methanol than the natural isoform, while the TS201S and G103L isoforms produced ~20% and ~70% lower fractions, respectively. The G103L isoform was also distinguished by producing the highest percentage of *exo*-3-norcaranol and the lowest percentage of cyclohex-2-enyl methanol. As with the natural enzyme, none of the T4moH isoforms yielded cyclohept-3-enol.

^{18}O Atom Incorporation with Norcarane. Previous studies of T4MO have shown that the O-atom transferred to *p*-cresol during the oxidation of toluene originates from O_2 with high fidelity (*63*). During the course of this work, this result was extended to studies of norcarane and other substrate analogues. Table 3 summarizes these results. When T4moH was reacted with norcarane in sealed reaction vials containing $^{18}O_2$, >95% of the total products derivatized with TMS-derivatizing reagent contained ^{18}O. As a complementary experiment, reactions containing ~85% enriched $^{18}OH_2$ and natural abundance O_2 gave low levels of ^{18}O incorporation (less than 1% with the variability attributable to error associated with low levels of background signal at the m/z value corresponding to ^{18}O incorporation). Therefore, O-atoms incorporated into the 2- and 3-norcaranols formed during T4MO-catalyzed hydroxylation of norcarane originate exclusively from O_2.

To investigate the origin of the O-atom found in cyclohex-2-enyl methanol, another norcarane oxidation was performed in a reaction vial containing partial enrichment in $^{18}O_2$. For this experiment, the norcarane reaction was allowed to proceed until sufficient product was obtained for effective analysis (7 min), and then toluene was added and converted to *p*-cresol in the exact same, sealed reaction mixture. These samples were extracted and subjected to GC/MS analysis without derivatization. Table 3 shows that the *p*-cresol obtained from this reaction had 65% enrichment in ^{18}O, which thus revealed the fraction of $^{18}O_2$ in the reaction vial. When the un-rearranged isomeric norcaranols isolated from this reaction vial were analyzed, 68% enrichment in ^{18}O was determined. Likewise, when cyclohex-2-enyl methanol was analyzed, 62% enrichment in ^{18}O was determined. Thus three monooxygenated products obtained from the same reaction had the same isotopic content as the O_2 utilized for catalysis. Most notably, this included the radical-rearranged cyclohex-2-enyl methanol.

Reaction of 1,1-Dimethylcyclopropane. The methylcyclopropanes are the smallest molecules available that give diagnostic products from oxidations involving either radical or cation intermediates. Frey and co-workers (*62*) used 1,1-DMCP (**5**) to show that both radical and cation oxidation products (3-methyl-3-buten-1-ol (**5B**) or 1-methylcyclobutanol (**5C**), respectively) were produced in an MmoH-catalyzed reaction. In contrast, results with P450s revealed only methyl hydroxylation (*37*), which could not directly yield further mechanistic information. We were interested to learn whether the smaller volume and less planar shape of 1,1-DMCP (calculated solvent-exposed surface area 363 Å^2) would allow products from both radical and cation

Table 2: Percentages of Products Observed during Enzyme Reactions with Norcarane[a]

hydroxylase	*endo*-2-norcaranol	*exo*-2- and *endo*-3-norcaranol	*exo*-3-norcaranol	**3D**	**3E**	lifetime (ps)	ref
T4moH	47.5 ± 0.4	39.2 ± 1.0	8.8 ± 0.3	4.5 ± 0.9	0	263 ± 55	this work
T201A	35.5 ± 1.1	48.5 ± 0.9	10.2 ± 1.3	5.8 ± 0.9	0	343 ± 55	
T201S	35.9 ± 1.2	50.4 ± 1.2	10.3 ± 1.2	3.5 ± 0.6	0	200 ± 30	
G103L	37.6 ± 0.8	49.8 ± 0.3	11.2 ± 0.9	1.4 ± 0.2	0	80 ± 11	
MMO (OB3b)	57	29	7	1.4	1.1	20	*41*
MMO (Bath)	53	29 and 6	3	3	2	*b*	*64*
AlkB	74	6		15	2	1000	*15*
$P450_{cam}$	56.7	19.8	9.1	0.9	0.3	52	*10*
$P450_{BM3}$	57.6	28.2	7.5	0.7	0.3	44	*10*
CYP2B4	68	21 and 4	4	3	4	*c*	*64*
CYPΔ2B4	70	21 and 4	4	0.4	0.5	*c*	*64*
CYP2B1	56.7	33.4	6.2	0.3	0.3	16	*10*
CYP2E1	31.7	60	5.7	0.6	*c*	35	*10*

[a] Determined by GC/MS analysis as described in Materials and Methods of this work or in the cited references. Standard deviations from T4moH oxidations were from three or more replicates, including different preparations of enzyme. [b] Not reported. Using the product distributions given in ref *64* and a norcaranyl radical lifetime of 2×10^8 s^{-1} from ref *15*, a lifetime of ~20 ps can be estimated. [c] Not determined.

Table 3: Origin of Oxygen Incorporated during T4MO Reactions[a]

substrate	product percentage	$^{18}O_2$ reactions	$^{18}OH_2$ reactions
	Toluene[b]		
p-cresol	96	>95	*c*
	Norcarane[d,e]		
total products	95.5	>95[f]	<1
	Norcarane/Toluene[g]		
un-rearranged	95.5	68	<1
radical-rearranged	4.5	62	<1
p-cresol	96	65[g]	*c*
	1,1-DMCP[d,e]		
un-rearranged	92.9	99.1 ± 0.8	0.9
radical-rearranged	0.2	79 ± 6	5.3
cation ring-expansion	2.1	69 ± 5	23 ± 2
unidentified product	4.8	99.4	0.3
	1,1-DECP[g]		
un-rearranged	89.7[h]	63.5 ± 0.5	10.6
radical-rearranged	1.8	65	7.3
cation ring-expansion	8.5	~1	91.3

[a] Reactions were performed as described in Materials and Methods. Standard deviations are the result of three or more separate determinations. [b] Product percentages from ref *52*; ^{18}O incorporation data from ref *63*. [c] Not determined. [d] The isotopic enrichment of the $^{18}O_2$ was 99%. [e] The reported percentage incorporation values were corrected for an 85% isotopic enrichment of ^{18}O in water. [f] Isotopic contents of combined 2- and 3-norcaranols. [g] The isotopic content of the $^{16}O_2/^{18}O_2$ mixture was determined experimentally to correspond to ~65% by reference to previous T4moH studies of *p*-cresol incorporation (*63*). [h] The reported percentage includes the contribution of corresponding ketone, ~17%.

oxidations, while the larger substrate norcarane was apparently unable to give a product characteristic of a cationic oxidation.

Figure 5 shows possible reaction pathways leading to the products observed from oxidation of 1,1-DMCP. In the presence of a saturated solution of 1,1-DMCP, T4moH gave $k_{cat} = 0.04$ s^{-1}. This was an ~50-fold decrease in rate relative to the physiological substrate toluene. Due to the low k_{cat} value and the qualitative association between k_{cat}, coupling, and substrate structure reported elsewhere (*51*, *52*), studies of k_{cat}/K_M and coupling efficiency were not undertaken. Figure 6 shows a GC/FID elution profile for the products obtained from this reaction. The un-rearranged product 1-methylcyclopropanemethanol (**5A**) represented ~93% of total products. This result is consistent with the hydroxylation reaction proceeding faster than the potential rearrangement or ring-expansion pathways indicated in Figure 5.

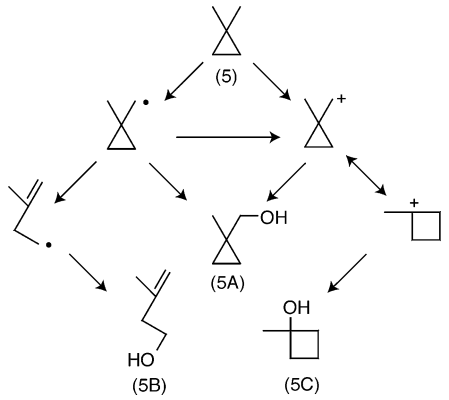

FIGURE 5: Reaction pathways of 1,1-dimethylcyclopropane (**5**) derived from either radical rearrangement or cation ring-expansion during oxidation at the methyl position. The un-rearranged hydroxylation product is 1-methylcyclopropanemethanol (**5A**). Rearrangement of a radical intermediate gives 3-methyl-3-buten-1-ol (**5B**), while ring expansion of a cation intermediate gives 1-methylcyclobutanol (**5C**).

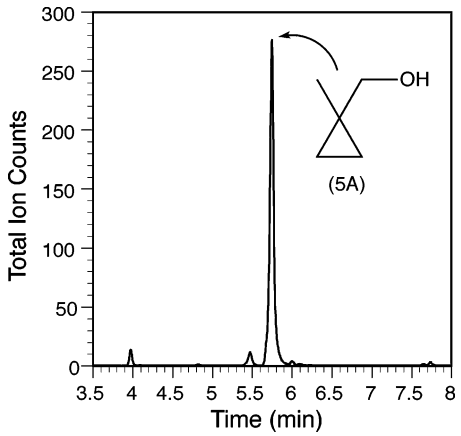

FIGURE 6: Representative GC elution profile of products obtained from T4MO-catalyzed reaction with 1,1-dimethylcyclopropane. The internal standard, 3-methylbenzyl alcohol, eluted at ~15.7 min and is not shown. The major product is 1-methylcyclopropanemethanol. A blank reaction was subtracted to give the chromatogram shown.

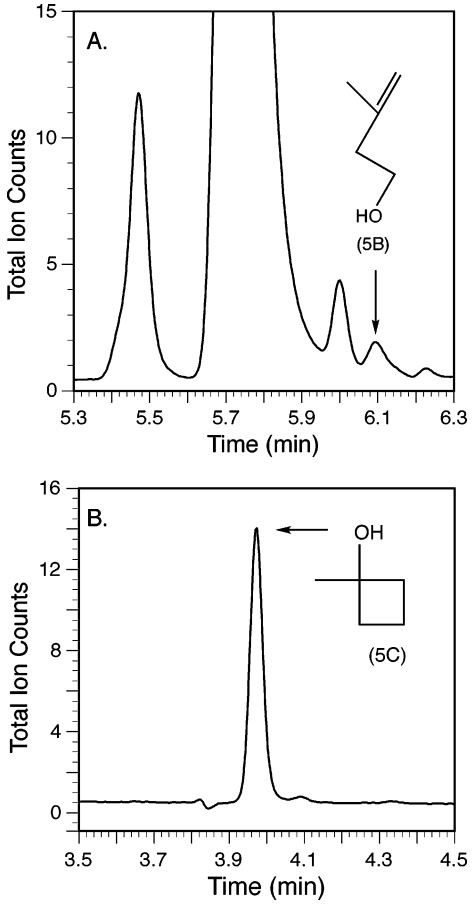

FIGURE 7: Expanded views of the elution profile from Figure 6: (A) elution profile from 3.5 to 4.5 min, showing elution of 1-methylcyclobutanol; (B0 elution profile from 5.3 to 6.3 min, indicating elution of 3-methyl-3-buten-1-ol. For clarity, the chromatograph obtained from the control sample was subtracted from the experimental chromatograph. The presence of unidentified products with elution times of 5.5 and 6.0 min was confirmed by GC/MS. A blank reaction was subtracted to give the chromatogram shown.

Figure 7 shows expanded scale representations of the GC profile from Figure 6. These profiles demonstrate the formation of both 3-methyl-3-buten-1-ol (**5B**, Figure 7A, ~0.2% of total products) and 1-methylcyclobutanol (**5C**, Figure 7B, ~2.1% of total products) during the T4moH-catalyzed reaction. These products have been previously assigned to arise from radical-rearrangement and cation ring-expansion reactions, respectively. The two additional unidentified peaks in Figure 7B, with 5.5 and 6.0 min elution times, accounted for 4.8% of the products. Both gave a time-dependent increase in intensity, suggesting that they might also be products of the enzyme reaction. However, these peaks did not correspond to the elution time of any of the other potential products listed in Materials and Methods and investigated in previous studies (*62*). Likewise, these peaks did not correspond to a secondary oxidation product as suggested by extended incubation of the majority product 1-methylcyclopropanemethanol with the active enzyme complex under turnover conditions.

O-Atom Incorporation with 1,1-Dimethylcyclopropane. Table 3 shows the results of 1,1-DMCP oxidations in $^{18}O_2$- and $^{18}OH_2$-enriched reaction mixtures. For reactions enriched in $^{18}O_2$ (99%), the un-rearranged 1-methylcyclopropanemethanol contained 99% of ^{18}O incorporated, matching the isotopic content of O_2 used. Interestingly, the two additional unidentified peaks also exhibited near complete fidelity for ^{18}O incorporation from $^{18}O_2$, suggesting they may be either an un-rearranged or a radical-rearranged alcohol. The isotopic content of the radical rearrangement product 3-methyl-3-buten-1-ol and the cation ring-expansion product 1-methylcyclobutanol was ~80% and ~70% enrichment in the incorporated O-atom, respectively.

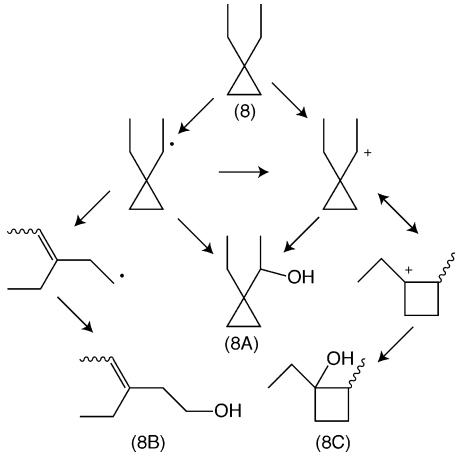

FIGURE 8: Reaction pathways of 1,1-diethylcyclopropane (**8**) derived from either radical rearrangement or cation ring expansion during oxidation at the secondary position of the ethyl group. The un-rearranged hydroxylation product is 1-ethylcyclopropaneethanol (**8A**). Rearrangement of a radical intermediate gives 3-methyl-3-penten-1-ol (**8B**), while ring expansion of a cation intermediate gives 1-methyl-2-ethylcyclobutanol (**8C**).

Oxidations of 1,1-DMCP performed in $^{18}OH_2$-enriched buffer provided a complementary result to the $^{18}O_2$ experiments (Table 3). Thus the un-rearranged and radical-rearranged products contained negligible amounts of ^{18}O incorporated from solvent (1−5%), while the cation ring-expansion product contained ~25% of ^{18}O enrichment derived from solvent. From these experiments, the un-rearranged and radical rearranged products from 1,1-DMCP appear to have an O-atom derived from O_2, while the cation ring-expansion product has an O-atom with an origin mixed between O_2 and H_2O.

Reaction of 1,1-Diethylcyclopropane. The mechanistically relevant reaction pathways available for 1,1-DECP can be understood by reference to Figure 8. In contrast to the primary C−H bond in 1,1-DMCP, 1,1-DECP (**8**) has a secondary C−H bond as the mechanistically relevant site of oxidation (as does norcarane). Furthermore, 1,1-DECP (calculated solvent-exposed surface area of 508 Å^2) is larger than 1,1-DMCP (363 Å^2), toluene (399 Å^2), and norcarane (471 Å^2) and is less planar than either toluene or norcarane owing to the tetrahedral arrangement of substituents around the quaternary carbon atom.

Figure 9 shows the GC profiles obtained from oxidation of 1,1-DECP. Steady-state kinetic studies showed that the k_{cat} of 1,1-DECP was closest to that of 1,1-DMCP, and the un-rearranged 1-(1-ethylcyclopropyl)-ethanol (and the corresponding ketone oxidation product) represented the majority of total products (**8A**, Figure 9, 89.7%). Furthermore, both 3-methyl-3-penten-1-ol (**8B**, Figure 9, ~1.8% of total products) and 1-methyl-2-ethylcyclobutanol (**8C**, Figure 9, 8.5% of total products) were observed from the T4moH-catalyzed reaction. By analogy to the assignments made for

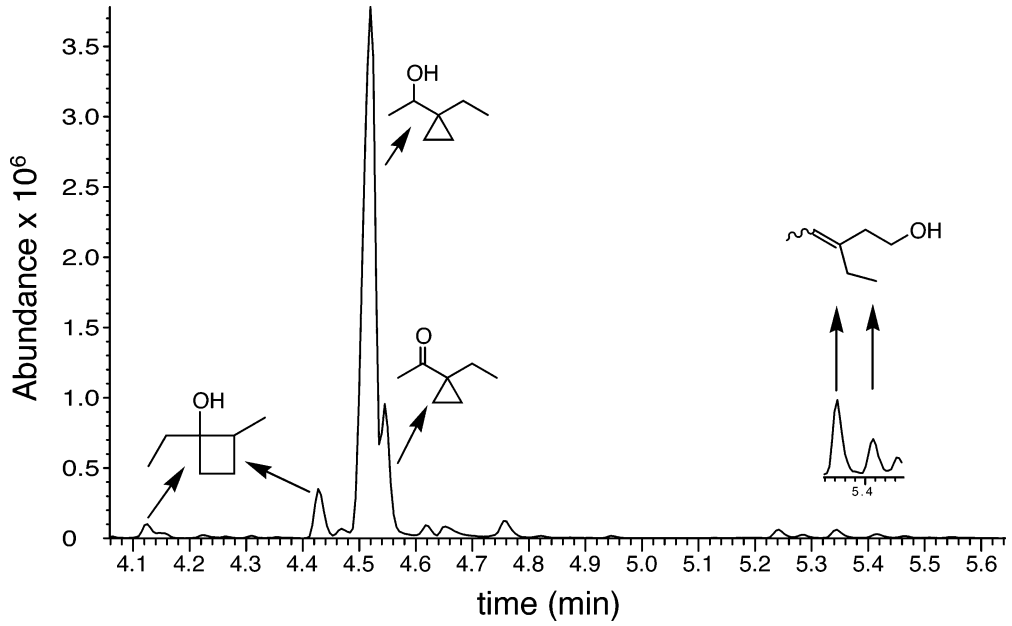

FIGURE 9: Representative GC elution profile of products obtained from T4MO-catalyzed reaction with 1,1-diethylcyclopropane. The major product is 1-(1-ethylcyclopropyl)-ethanol (and the corresponding ketone oxidation product). The elution times of two isomers of cation ring-expansion product 1-methyl-2-ethylcyclobutanol are indicated. The elution times of two isomers of radical rearranged product 3-methyl-3-penten-1-ol are also indicated and shown with an expanded vertical scale in the inset.

1,1-DMCP, these products are assigned to arise from radical-rearranged and cation ring-expansion intermediates, respectively. Relative to the products obtained from 1,1-DMCP, the altered shape of 1,1-DECP, the weakened strength of the mechanistically relevant secondary C−H bond, and the increased stability of a secondary carbocation apparently led to the increase in both of these products.

Table 3 summarizes O-atom incorporation experiments with 1,1-DECP. When the oxidation of 1,1-DECP was performed in $^{18}O_2$, the radical-rearranged product contained the same enrichment in ^{18}O as the un-rearranged product, while the cation ring-expansion product contained only ~1% enrichment. For comparison, reaction in $^{18}OH_2$ gave only ~10% enrichment of ^{18}O in the un-rearranged and radical-rearranged products, while the cation product contained ~90% enrichment in ^{18}O. Therefore, the un-rearranged and radical rearranged products obtained from 1,1-DECP have an O-atom derived from O_2, while the cation ring-expansion product has an O-atom derived from H_2O.

DISCUSSION

In this work, four T4moH isoforms have been used to study the possible influence of the active site on the reaction outcome with the diagnostic substrate norcarane. The results reveal comparable k_{cat} values and coupling efficiencies for oxidation of norcarane and toluene, the natural substrate. This comparable reactivity in steady-state catalysis has not been generally established with other "radical-clock" analogues.[2] The overall similarities in the shapes of norcarane and toluene (Figure 2) suggest the two molecules bind in the T4moH active site in a similar manner and thus maintain crucial enzyme−substrate interactions and distance constraints during catalysis.

Chemical Reactions of Norcarane. Figure 3 shows reaction pathways for norcarane originating with either a C-2 radical (**3A**) or a C-2 cation (**3B**). **3A** may arise by $1e^-$ oxidation of norcarane, while **3B** may arise by a direct $2e^-$ oxidation, by a second $1e^-$ oxidation of **3A**, or by a solvolytic reaction involving a protonated norcaranol. The insertion of [$^+$OH] into the C−H bond, as indicated in Figure 1C, would provide a mechanism for generation of a protonated norcaranol required for the solvolytic reaction, as would intrinsic Lewis or Bronsted acidity at the active site. In the latter scenario, cation formation would occur after the initial formation of a product alcohol. As discussed elsewhere, if formation of a C-2 cation can lead to formation of a cyclohex-2-enylmethyl cation, the distinction between radical and cation reaction manifolds may become uncertain (*64*). Therefore, the relative contributions of these different oxidation manifolds to the formation of **3D** are central to the recent differences in conclusions derived from studies of norcarane oxidation by methane monooxygenase (*41*, *64*) and cytochrome P450 (*10*).

Chemical studies of the solvolysis of norcaranol have been reported. For example, acetolysis of 2-deuterio-2-norcaranol (*64*) gave predominant formation of cyclohept-3-enol (**3E**, 96%) and a minor fraction of cyclohex-2-enyl methanol (**3D**, 4%). Furthermore, solvolysis of 2-norcaranol−dinitrobenzoate esters (*64*) gave a mixture of *endo*- and *exo*-2-norcaranols (~90%) and the ring-expansion product **3E** (~10%), while no rearrangement product **3D** was detected. Likewise, solvolysis of the tosylate of cyclohex-2-enyl methanol gave a mixture of products with 2-norcaranol and **3E** representing the majority consitutents (*10*). These results apparently reflect the higher stability of the secondary carbocation produced by ring expansion as compared to rearrangement to a primary carbocation as the precursor to **3D**. Thus the preponderance of chemical evidence shows that

[2] A transient kinetics study of the reaction of norcarane with *Methylosinus trichosporium* OB3b MmoH showed that the rates of all phases measured, including formation of the high-valent oxidant compound Q and its dissipation in the C−H bond oxidation step, were roughly comparable to that observed for methane (*41*).

solvolytic reactions of norcaranol give rise to a majority of cation ring-expansion product. Indeed, only a minor fraction of rearranged cyclohex-2-enyl methanol should be anticipated from the results of the chemical solvolysis studies. These chemical findings contrast with the exclusive formation of cyclohex-2-enyl methanol from the T4moH reaction, implicating a radical intermediate in formation of this product.

Structural Alignments of Toluene, Norcarane, and Products. Figure 2, middle panel, shows a stereo overlay of norcarane and cyclohex-2-enyl methanol. In the rearranged product, the bridgehead carbon has moved ~1.5 Å from the original position in the aligned norcarane. As a consequence, the methanol group of cyclohex-2-enyl methanol has moved into closer correspondence to the position that the methyl group of toluene might occupy in the active site. Moreover, the inserted −OH group is within 3.3 Å of the 2-*endo*-hydrogen removed in the oxidation.

Figure 2, bottom panel, shows a stereo overlay of norcarane and cyclohept-3-enol, a product derived from cation-initiated ring expansion of norcarane during oxidation reactions. The loss of the bicyclic structure causes an overall increase in the size of the ring. Furthermore, the −OH group would reside on the opposite side of the product and greater than 4.5 Å distant from the 2-*endo*-hydrogen removed from the aligned norcarane.

T4moH-Catalyzed Oxidation of Norcarane. The results show that reaction of T4moH and three additional catalytically competent isoforms gave only cyclohex-2-enyl methanol (**3D**) as a diagnostic product. We propose that the simplest mechanism consistent with formation of this product is the rearrangement of a radical intermediate generated during the oxidation reaction followed by transfer of an O-atom derived from O_2.

By the alternative assumption that either $2e^-$ oxidation or solvolysis provided a 2-norcaranyl cation, the present results would require that the active site exclusively promote the conversion of this intermediate into the cyclohex-2-enylmethyl cation precursor of **3D**. This active site capability would contradict the predominance of the ring-opened cyclohept-3-enyl cation formed in the chemical solvolysis experiments described above. Of course, this preference might be achieved by invoking close binding interactions that inhibit the ring expansion required to form the cyclohept-3-enyl cation. However, the level of ^{18}O incorporation in the cyclohex-2-enyl methanol recovered from the T4moH reaction (essentially matching the isotopic enrichment in O_2, Table 3) would also require that this cation must only react with either the stoichiometric water produced within the active site during the monooxygenase reaction or the O_2-derived, iron-bound oxo-oxygen. These restrictions have strong implications for the mechanism, geometry or both of reaction and will be more fully examined along with the patterns for isotopic labeling of radical- and cation-derived products from other probe molecules in the O-Atom Incorporation Results, see below.

Reactions of Other Enzymes with Norcarane. Table 2 summarizes results obtained from the oxidation of norcarane by various enzyme systems. From these studies, there is considerable variability in the distribution of the unrearranged 2-norcaranol isomers and in the percentage of cyclohex-2-enyl methanol (**3D**). In combination with the varied regiospecificities of the T4moH isoforms, Table 2 confirms the influence of the active site on the outcome of reaction with norcarane.

The mutated isoforms of T4moH used in this study were created to address the role of a conserved hydrogen-bond donor in the active site (T201, *54*) and to explore the origin of regiospecificity (G103, *52*). We have previously shown that T4moH does not require conserved Thr201 during steady-state aromatic hydroxylation reactions (*54*), and this work shows that Thr201 is not essential for alkane hydroxylation reactions either. In contrast, studies on T4moH (*51, 52, 54*), toluene 2-monooxygenase (*65*−*67*), and ribonucleotide reductase (*68*−*73*) have shown that the residues near to FeA (such as G103 in T4moH) have a substantial impact on the outcome of catalysis including changes in regiospecificity and stability of diiron center intermediates.

The k_{cat} values of the T4moH isoforms exhibit the same ~1.3-fold variation for oxidation of either toluene or norcarane, suggesting that similar factors may control catalysis with these electronically distinct substrates. For example, steric interactions may modify the trajectory of approach required for orbital overlap and bond cleavage, alter the rates of enzyme conformational change presumed to be required for conversion between intermediates, or interfere with motions of substrate intermediates required to complete the O-atom transfer reaction. In addition, the chemical properties of the oxidant may favor either $1e^-$ or $2e^-$ oxidation pathways or the generation of $[OH^+]$ during the reaction, while chemical properties of the substrate may also contribute to the favorability of these different options.

T4moH-Catalyzed Oxidation of Cyclopropanes. Figure 7 shows that T4moH gives both rearrangement and ring expansion during the oxidation of 1,1-DMCP. The appearance of the rearranged 3-methyl-3-buten-1-ol is considered diagnostic for a radical intermediate, while the expanded 1-methylcyclobutanol is characteristic of a cation intermediate. These products offer further insight into the reactivity of T4moH. The rearrangement rates for the cyclopropylcarbinyl radicals of 1,1-DMCP and 1,1-DECP [0.8×10^8 and 0.5×10^8 s^{-1}, respectively (*44*)] are slower than that for the 2-norcaranyl radical [2×10^8 s^{-1} (*15*)]. This is consistent with the lesser fraction of the radical-rearranged products obtained from 1,1-DMCP and 1,1-DECP oxidations relative to the radical-rearranged product obtained from norcarane.

For both 1,1-DMCP and 1,1-DECP, control reactions demonstrated that acidic conditions and heat could stimulate conversion between un-rearranged alcohols and cyclobutanols, and it is reasonable to assign these results to solvolysis reactions. It is also notable that the acidic conditions did not yield the rearranged alcohol products associated with radical intermediates. Further investigations of reaction workup conditions (see Materials and Methods) revealed that neither 1-methylcyclobutanol (**5C**) nor 1-ethyl-2-methylcyclobutanol (**8C**) were produced in the enzyme reaction buffer in the absence of the active enzyme, and likewise, the cation ring-expansion products were not produced by the mild extraction conditions used for workup of the enzyme reaction products. Thus the cyclobutanol products obtained with T4moH are attributed to the consequences of enzyme activity.

O-Atom Incorporation Results. A diiron monooxygenase active site provides an organized and accurately dimensioned

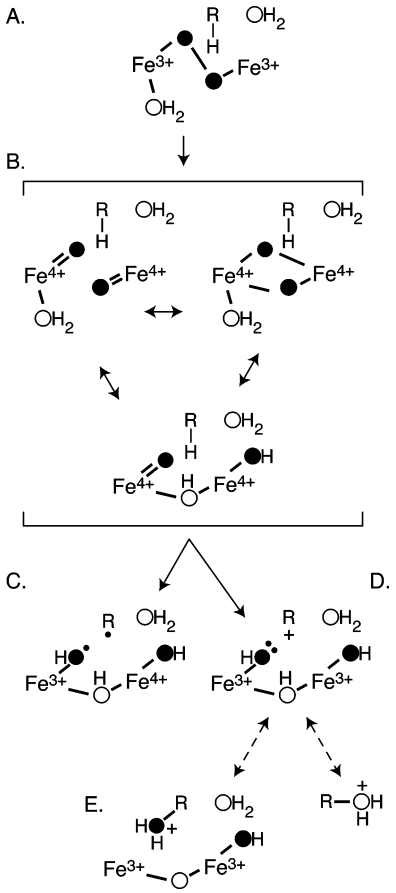

FIGURE 10: A schematic representation of O-atoms in the diiron hydroxylase active site.[3] The black spheres represent O-atoms derived from O_2 that may be either incorporated into substrate or converted to water or hydroxide according to the monooxygenase reaction stoichiometry. The open spheres represent solvent water sequestered in the active site. Oxidized substrate intermediates potentially have access to each of these three different types of O-atoms: (A) peroxodiferric intermediate; (B) three plausible representations of compound Q; (C) a $1e^-$ oxidation of substrate by compound Q to generate a substrate radical with a rebound reaction giving rise to the hydroxylated product; (D) a $2e^-$ oxidation of substrate by compound Q to generate a substrate cation, which can potentially react with any water present in the active site; (E) putative proton transfer from an active site acid to generate a protonated alcohol capable of undergoing solvolysis and recombination with active site water.

space where catalysis must proceed. The high-fidelity O-atom transfer observed with diiron enzymes (reported here and elsewhere (*62*, *63*, *74*)), the identities of residues that alter regiospecificity of T4moH hydroxylation reactions (*51*, *52*), the positional specificity of chain cleavage observed with acyloxy- and thiastearoyl-ACPs by stearoyl-ACP desaturase (*75*, *76*), and the location of the Tyr122 radical formed by ribonucleotide reductase (*77*) all indicate that a specific iron atom will be the leading oxidant in the diiron enzymes.

Figure 10 shows the different types of O-atoms that might be incorporated in a diiron monooxygenase reaction, in this case assuming breakage of the peroxo O−O bond leading to three plausible formulations of compound Q, the oxidizing intermediate (*78*).[3] Along with the electrophilic oxygen transferred from the diiron center to the hydrocarbon substrate, a water molecule must be generated from the stoichometry of the monooxygenase reaction. These two oxygen atoms (black spheres) will likely reside close to the diiron center and the substrate during the oxidation reaction. Furthermore, it is likely that other solvent-derived water molecules (white spheres) will be found in the active site (either bound to the diiron center or located in other positions), and these may reside at a range of distances from the center of reaction.

Radical and cation intermediates will have different propensities for reaction with these different types of O-atoms. For example, the spin-paired recombination of radicals (Figure 10C) and the reaction of a carbocation with water (Figure 10D) are well established. Indeed, the isotopic incorporation studies presented here show that the different classes of product molecules have different types of O-atom incorporated, that is, the un-rearranged and radical-rearranged products contain high-level enrichment of an O-atom derived from O_2 (see Table 3). In contrast, the cation ring-expansion products observed with 1,1-DMCP and 1,1-DECP contain variable enrichment of an O-atom derived from water. Since the monooxygenase reaction also creates water in close proximity in the active site but at a distinct position relative to the initial site of oxidation, the degree to which a substrate cation can discriminate between the water of reaction and solvent water will influence the isotopic content of the cation ring-expansion products.

The isotopic content of 1-methylcyclobutanol provides evidence for this discrimination, as ~70% of the oxygen in this product is derived from either O_2 or the water of reaction while 25% comes from solvent water. This result also corresponds with the partial isotopic incorporation observed in reactions performed in $^{18}OH_2$ (~25% of isotopic enrichment), where capture of the water of reaction derived from $^{16}O_2$ would lead to a depressed level of ^{18}O incorporation from $^{18}OH_2$ solvent. Consequently, geometric considerations of the diiron enzyme active site may place the 1-methylcyclobutyl cation in a favorable position for recombination with the water of reaction. In contrast, the cation ring-expansion product from 1,1-DECP had essentially no ^{18}O incorporation from $^{18}O_2$ and complete incorporation from $^{18}OH_2$ derived from the medium. These results indicate that the cation arising from oxidation of 1,1-DECP must have access to an alternative position in the active site that favors recombination with solvent water and not with the water of reaction or the iron-bound oxo-oxygen. Whether this cation arises from $2e^-$ oxidation of the substrate before O-atom transfer (Figure 10D) or from solvolysis of a protonated alcohol formed in the active site (Figure 10E) cannot be ascertained from these experiments.

Mechanism Considerations. For natural T4moH, the mechanism of *p*-cresol formation has been proposed to include a directed approach of toluene to the diiron oxidant, formation of a transient 3,4-arene oxide, and active site-directed opening of the arene oxide to the final product (*55*). Figure 11A summarizes this mechanistic proposal. Figure 11B suggests that norcarane may also experience a similar

[3] The disposition of an electrophilic oxo-metal intermediate, the water of reaction, and active site water can be considered for other monooxygenase reactions. For example, heterolytic cleavage of a terminal metallohydroperoxo, as proposed for P450 catalysis (*8*), would generate the oxo-metal oxidant and release the water of reaction into the active site. This would be distinct from reaction of a bridging peroxo intermediate as in the diiron hydroxylases, where both O-atoms from O_2 may remain bound to iron during the oxidation reaction.

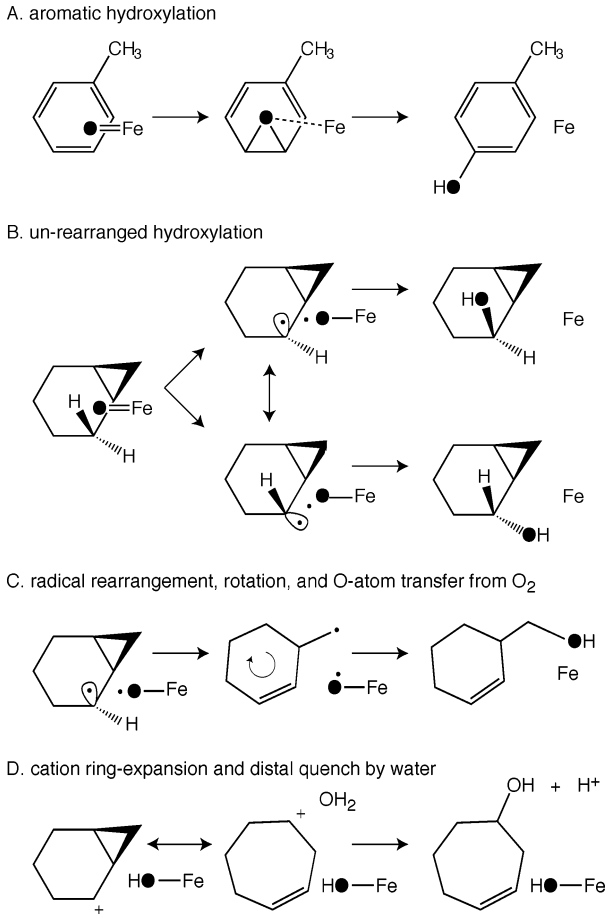

FIGURE 11: Proposed mechanisms for reaction of T4moH with aromatics and alkanes: (A) reaction with toluene via formation of a transient 3,4 arene oxide (*55*); (B) reaction at the C-2 position of norcarane leading to the corresponding *endo*-2- and *exo*-2-norcaranols; the stereospecificity of C−H abstraction and the role of epimerization in determining the final product distribution are not known; (C) a $1e^-$ oxidation of norcarane, rearrangement of the 2-norcaranyl radical, and rotation of the cyclohex-2-enyl-methyl radical prior to O-atom transfer and formation of the rearrangement product cyclohex-2-enyl methanol; (D) plausible resonance hybrid between 2-norcaranyl cation and cycloheptenyl cation that may react with active site water to yield cyclohept-3-enol. This product is not observed from T4moH-catalyzed reactions.

trajectory of approach to the diiron oxidant and orientation within the active site. This suggestion is compatible with the structural similarity of norcarane and toluene shown in Figure 2 and may give rise to a majority oxidation at C-2 of norcarane to account for the product distributions presented in Table 2. As outlined in Figure 3, T4MO-catalyzed reaction at C-2 gives rise to isomeric norcaranols and to cyclohex-2-enyl methanol, both having an ^{18}O content indistinguishable from $^{18}O_2$. Figure 11B,C also suggests that the relative positions of the C-2 radical and diiron oxidant relative to the bridgehead carbon (which is ultimately hydroxylated in the radical-rearranged product) may contribute to the favorability of O-atom transfer as opposed to radical rearrangement prior to O-atom transfer. Conceivably, the marked 70% decrease (see Table 2) in the amount of rearranged product observed with the G103L isoform may be a manifestation of the enhanced reactivity of this isoform at the 2,3-position of toluene, which better corresponds to the C-2 position of the aligned norcarane shown in Figure 2, top panel.

The minimum distance between abstracted hydrogen atom and carbon atom that will receive the transferred O-atom (95% enrichment in ^{18}O from $^{18}O_2$) is 2.8 Å. This long distance is suggestive that partial rotation of the substrate relative to the oxidant (as indicated in Figure 11C) may be required to achieve the high fidelity observed for O-atom transfer.

Figure 11D diagrams a cation ring-expansion reaction leading to the formation of cyclohept-3-enol, a product that was not observed from the T4moH reactions. The minimum distance between the abstracted hydrogen atom and carbon atom that would receive the transferred O-atom is 4.9 Å. Moreover, this carbon atom lies on the opposite side of the substrate, as it would be oriented in the active site. These geometric considerations suggest that substantial motion might be required to incorporate an O-atom from O_2 and instead an O-atom from solvent might be incorporated with high efficiency into this product.

Once less-well-matched substrates such as 1,1-DMCP and 1,1-DECP were introduced into the T4moH reaction, the product distribution expanded to include un-rearranged, radical-rearranged, and cation ring-expansion products. These different classes of products undoubtedly arise from alternative binding configurations available relative to a strong oxidant and intrinsic differences in the chemical properties of the substrates. It is reasonable to conclude that small adjustments of the orientations and distances between substrates, intermediates, and oxidants can have profound influence on the favorability of $1e^-$, $2e^-$, and O-atom transfer reactions.

CONCLUSIONS

These studies have implicated the formation of both radical and cation intermediates during the hydroxylations of diagnostic hydrocarbon substrate probes by T4moH. The relative amounts of radical-rearranged alcohols correlated with the radical rearrangement rate constant, since norcarane, with the fastest ring-opening rate constant, showed the most radical-pathway product. The relative amount of cation products seems to be related to the ease of cation formation from the product alcohols. Further, the radical and cation reaction pathways have been dissected by observing the capture of different oxygen pools by the two intermediates, in accord with their chemical reactivity.

ACKNOWLEDGMENT

B.G.F. and L.A.M. thank Prof. P. A. Frey (University of Wisconsin) for generously providing samples of 1,1-DMCP, 1-methylcyclopropanemethanol, and 1-methylcyclobutanol used to initiate these studies. R.N.A. and J.T.G. thank the Environmental Molecular Science Institute CEBIC at Princeton University.

REFERENCES

1. Kelly, S. L., Lamb, D. C., Jackson, C. J., Warrilow, A. G., and Kelly, D. E. (2003) The biodiversity of microbial cytochromes P450, *Adv. Microb. Physiol. 47*, 131−186.
2. Sullivan, J. P., Dickinson, D., and Chase, H. A. (1998) Methanotrophs, *Methylosinus trichosporium* OB3b, sMMO, and their application to bioremediation, *Crit. Rev. Microbiol. 24*, 335−373.
3. Knief, C., Lipski, A., and Dunfield, P. F. (2003) Diversity and activity of methanotrophic bacteria in different upland soils, *Appl. Environ. Microbiol. 69*, 6703−6714.

4. Shively, J. M., English, R. S., Baker, S. H., and Cannon, G. C. (2001) Carbon cycling: the prokaryotic contribution, *Curr. Opin. Microbiol. 4*, 301−306.
5. Williams, P. A., and Sayers, J. R. (1994) The evolution of pathways for aromatic hydrocarbon oxidation in *Pseudomonas*, *Biodegradation 5*, 195−217.
6. Gottschalk, G. (1986) in *Bacterial Metabolism*, p 359, Springer-Verlag, New York.
7. Ortiz de Montellano, P. R. (2004) in *Cytochrome P450: Structure, Mechanism, and Biochemistry* (Ortiz de Montellano, P. R., Ed.), in press, Kluwer Academic/Plenum Press, New York.
8. Groves, J. T. (2004) Models and Mechanisms of Cytochrome P450 Action in *Cytochrome P450: Structure, Mechanism, and Biochemistry* (Ortiz de Montellano, P. R., Ed.) pp 1−44, Kluwer Academic/Plenum Press, New York.
9. Groves, J. T. (2003) The bioinorganic chemistry of iron in oxygenases and supramolecular assemblies, *Proc. Natl. Acad. Sci. U.S.A. 100*, 3569−3574.
10. Auclair, K., Hu, Z., Little, D. M., Ortiz de Montellano, P. R., and Groves, J. T. (2002) Revisiting the mechanism of P450 enzymes with the radical clocks norcarane and spiro[2,5]octane, *J. Am. Chem. Soc. 124*, 6020−6027.
11. Wallar, B. J., and Lipscomb, J. D. (1996) Dioxygen activation by enzymes containing binuclear non-heme iron clusters, *Chem. Rev. 96*, 2625−2657.
12. Kopp, D., and Lippard, S. J. (2002) Soluble methane monooxygenase: activation of dioxygen and methane, *Curr. Opin. Chem. Biol. 6*, 568−576.
13. Baik, M.-H., Newcomb, M., Freisner, R. A., and Lippard, S. J. (2003) Mechanistic studies on the hydroxylation of methane by methane monooxygenase, *Chem. Rev. 103*, 2385−2419.
14. Austin, R. N., Buzzi, J., Kim, E., Zylstra, G. J., and Groves, J. T. (2003) Xylene monooxygenase: a membrane-spanning non-heme diiron enzyme that hydroxylates hydrocarbons via a substrate radical intermediate, *J. Biol. Inorg. Chem. 8*, 733−740.
15. Austin, R. N., Chang, H.-K., Zylstra, G. J., and Groves, J. T. (2000) The non-heme diiron alkane monooxygenase of Pseudomonas oleovorans (AlkB) hydroxylates via a substrate radical intermediate, *J. Am. Chem. Soc. 122*, 11747−11748.
16. Shanklin, J., Achim, C., Schmidt, H., Fox, B. G., and Münck, E. (1997) Mössbauer studies of alkane ω-hydroxylase: Evidence for a diiron cluster in an integral membrane enzyme, *Proc. Natl. Acad. Sci. U.S.A. 94*, 2981−2986.
17. Lemos, S. S., Collins, M. L. P., Eaton, S. S., Eaton, G. R., and Antholine, W. E. (2000) Comparison of EPR-visible Cu^{2+} sites in pMMO from Methylococcus capsulatus (Bath) and Methylmicrobium album BG8, *Biophys. J. 79*, 1085−1094.
18. Murrell, J. C., McDonald, I. R., and Gilbert, B. (2000) Regulation of expression of methane monooxygenases by copper ions, *Trends Microbiol. 8*, 221−225.
19. Chan, S. I., Chen, K. H. C., Yu, S. S. F., Chen, C. L., and Kuo, S. S. J. (2004) Toward delineating the structure and function of the particulate methane monooxygenase from methanotrophic bacteria, *Biochemistry 43*, 4421−4430.
20. Yu, S. S. F., Wu, L. Y., Chen, K. H. C., Luo, W. I., Huang, D. S., and Chan, S. I. (2003) The stereospecific hydroxylation of [2,2-H-2(2)]butane and chiral dideuteriobutanes by the particulate methane monooxygenase from *Methylococcus capsulatus* (Bath), *J. Biol. Chem. 278*, 40658−40669.
21. Lieberman, R. L., Shrestha, D. B., Doan, P. E., Hoffman, B. M., Stemmler, T. L., and Rosenzweig, A. C. (2003) Purified particulate methane monooxygenase from *Methylococcus capsulatus* (Bath) is a dimer with both mononuclear copper and a copper-containing cluster, *Proc. Natl. Acad. Sci. U.S.A. 100*, 3820−3825.
22. Basu, P., Katterle, B., Andersson, K. K., and Dalton, H. (2003) The membrane-associated form of methane monooxygenase from *Methylococcus capsulatus* (Bath) is a copper/iron protein, *Biochem. J. 369*, 417−427.
23. Choi, D. W., Kunz, R. C., Boyd, E. S., Semrau, J. D., Antholine, W. E., Han, J. I., Zahn, J. A., Boyd, J. M., de la Mora, A. M., and DiSpirito, A. A. (2003) The membrane-associated methane monooxygenase (pMMO) and pMMO−NADH:quinone oxidoreductase complex from *Methylococcus capsulatus* (Bath), *J. Bacteriol. 185*, 5755−5764.
24. Shaik, S., de Visser, S. P., Ogliaro, F., Schwarz, H., and Schroder, D. (2002) Two-state reactivity mechanisms of hydroxylation and epoxidation by cytochrome P-450 revealed by theory, *Curr. Opin. Chem. Biol. 6*, 556−567.
25. Groves, J. T., and McCluskey, G. A. (1976) Aliphatic hydroxylation via oxygen rebound: Oxygen transfer catalyzed by iron, *J. Am. Chem. Soc. 98*, 859−861.
26. Rataj, M. J., Knauth, J. E., and Donnelly, M. I. (1991) Oxidation of deuterated compounds by high specific activity methane monooxygenase from *Methylosinus trichosporium* OB3b, *J. Biol. Chem. 266*, 18684−18690.
27. Nesheim, J. C., and Lipscomb, J. D. (1996) Large kinetic isotope effects in methane oxidation catalyzed by methane monooxygenase: Evidence for C−H bond cleavage in a reaction cycle intermediate, *Biochemistry 35*, 10240−10247.
28. Priestly, N. D., Floss, H. D., Froland, W. A., Lipscomb, J. D., Williams, P. G., and Morimoto, H. (1992) Cryptic stereochemistry of the methane monooxygenase reaction, *J. Am. Chem. Soc. 114*, 7561−7562.
29. Valentine, A. M., Wilkinson, B., Liu, K. E., Komar-Panicucci, S., Priestly, N. D., Williams, P. D., Morimoto, H., Floss, H. G., and Lippard, S. J. (1997) Tritiated chiral alkanes as substrates for soluble methane monooxygenase from *Methylococcus capsulatus* (Bath): Probes for the mechanism of hydroxylation, *J. Am. Chem. Soc. 119*, 1818−1827.
30. Wilkins, P. C., Dalton, H., Samuel, C. J., and Green, J. (1994) Further evidence for multiple pathways in soluble methane-monooxygenase-catalysed oxidations from the measurement of deuterium kinetic isotope effects, *Eur. J. Biochem. 226*, 555−560.
31. Dunietz, B. D., Beachy, M. D., Cao, Y., Whittington, D. A., Lippard, S. J., and Friesner, R. A. (2000) Large scale ab initio quantum chemical calculation of the intermediates in the soluble methane monooxygenase catalytic cycle, *J. Am. Chem. Soc. 122*, 2828−2839.
32. Guallar, V., Gherman, B. F., Miller, W. H., Lippard, S. J., and Friesner, R. A. (2002) Dynamics of alkane hydroxylation at the non-heme diiron center in methane monooxygenase, *J. Am. Chem. Soc. 124*, 3377−3384.
33. Musaev, D. G., Basch, H., and Morokuma, K. (2002) Theoretical study of the mechanism of alkane hydroxylation and ethylene epoxidation reactions catalyzed by diiron bis-oxo complexes. The effect of substrate molecules, *J. Am. Chem. Soc. 124*, 4135−4148.
34. Siegbahn, P. E. (2001) O−O bond cleavage and alkane hydroxylation in methane monooxygenase, *J. Biol. Inorg. Chem. 6*, 27−45.
35. Siegbahn, P. E. M., and Crabtree, R. H. (1997) Mechanism of C−H activation by diiron methane monooxygenases: Quantum chemical studies, *J. Am. Chem. Soc. 119*, 3103−3113.
36. Stearns, R. A., and Ortiz de Montellano, P. R. (1985) Cytochrome P-450 catalyzed oxidation of quadricyclane. Evidence for a radical cation intermediate, *J. Am. Chem. Soc. 107*, 4081−4082.
37. Ortiz de Montellano, P. R., and Stearns, R. A. (1987) Timing of the radical recombination step in cytochrome P-450 catalysis with ring-strained probes, *J. Am. Chem. Soc. 109*, 3415−3420.
38. Choi, S.-Y., Eaton, P. E., Kopp, D. A., Newcomb, M., Lippard, S. J., and Shen, R. (1999) Cationic species can be produced in soluble methane monooxygenase-catalyzed hydroxylation reactions; radical intermediates are not, *J. Am. Chem. Soc. 121*, 12198−12199.
39. Newcomb, M., and Toy, P. H. (2000) Hypersensitive radical probes and the mechanisms of cytochrome P450-catalyzed hydroxylation reactions, *Acc. Chem. Res. 33*, 449−455.
40. Newcomb, M., Shen, R., Choi, S.-Y., Toy, P. H., Hollenberg, P. F., Vaz, A. D. N., and Coon, M. J. (2000) Cytochrome P450-catalyzed hydroxylation of mechanistic probes that distinguish between radicals and cations. Evidence for cationic but not for radical intermediates, *J. Am. Chem. Soc. 122*, 2677−2686.
41. Brazeau, B. J., Austin, R. N., Tarr, C., Groves, J. T., and Lipscomb, J. D. (2001) Intermediate Q from soluble methane monooxygenase hydroxylates the mechanistic substrate probe norcarane: evidence for a stepwise reaction, *J. Am. Chem. Soc. 123*, 11831−11837.
42. Griller, D., and Ingold, K. U. (1980) Free-radical clocks, *Acc. Chem. Res. 13*, 317−323.
43. Ingold, K. U., and Walton, J. C. (1986) Small, strained bicycloalkyl radicals and some homolytic reactions involving their parent bicycloalkanes, *Acc. Chem. Res. 19*, 72−77.
44. Bowry, V. W., Lustzk, J., and Ingold, K. U. (1991) Calibration of a new horology of fast radical "clocks". Ring-opening rates for ring- and α-alkyl-substituted cyclopropylcarbinyl radicals and for the bicyclo[2.1.0]pent-2-yl radical, *J. Am. Chem. Soc. 113*, 5687−5698.

45. Bowry, V. W., Lusztyk, J., and Ingold, K. U. (1989) Calibration of the bicyclo[2.1.0]pent-2-yl radical ring opening and an oxygen rebound rate constant for cytochrome P-450, *J. Am. Chem. Soc. 111*, 1927−1928.
46. Choi, S.-Y., Eaton, P. E., Hollenberg, P. F., Liu, K. E., Lippard, S. J., Newcomb, M., Putt, D. A., Upadhyaya, S., and Xiong, Y. (1996) Regiochemical variations in reactions of methylcubane with *tert*-butoxyl radical, cytochrome P-450 enzymes, and a methane monooxygenase system, *J. Am. Chem. Soc. 118*, 6547−6555.
47. Pikus, J. D., Studts, J. M., Achim, C., Kauffmann, K. E., Münck, E., Steffan, R. J., McClay, K., and Fox, B. G. (1996) Recombinant toluene 4-monooxygenase: Catalytic and Mössbauer studies of the purified diiron and Rieske components of a four-protein complex, *Biochemistry 35*, 9106−9119.
48. Whited, G. M., and Gibson, D. T. (1991) Separation and partial characterization of the enzymes of the toluene-4-monooxygenase catabolic pathway in *Pseudomonas mendocina* KR1, *J. Bacteriol. 173*, 3017−3020.
49. McClay, K., Fox, B. G., and Steffan, R. J. (1996) Chloroform mineralization by toluene-oxidizing bacteria, *Appl. Environ. Microbiol. 62*, 2716−2722.
50. McClay, K., Fox, B. G., and Steffan, R. J. (2000) Toluene monooxygenase catalyzed epoxidation of alkenes, *Appl. Environ. Microbiol. 66*, 1877−1882.
51. Pikus, J. D., Studts, J. M., McClay, K., Steffan, R. J., and Fox, B. G. (1997) Changes in the regiospecificity of aromatic hydroxylation produced by active site engineering in the diiron enzyme toluene 4-monooxygenase, *Biochemistry 36*, 9283−9289.
52. Mitchell, K. H., Studts, J. M., and Fox, B. G. (2002) Combined participation of effector protein binding and hydroxylase active site residues provide toluene 4-monooxygenase regiospecificity, *Biochemistry 41*, 3176−3188.
53. Groves, J. T., Kruper, J. W., and Haushalter, R. C. (1980) Hydrocarbon oxidation with oxometalloporphinates. Isolation and reaction of a (porphinato)manganese(V) complex, *J. Am. Chem. Soc. 102*, 6375−6377.
54. Pikus, J. D., Mitchell, K. H., Studts, J. M., McClay, K., Steffan, R. J., and Fox, B. G. (2000) Threonine 201 in the diiron enzyme toluene 4-monooxygenase is not required for catalysis, *Biochemistry 39*, 791−799.
55. Mitchell, K. H., Rogge, C. E., Gierahn, T., and Fox, B. G. (2003) Insight into the mechanism of aromatic hydroxylation by toluene 4-monooxygenase through the use of specificially deuterated toluene and *p*-xylene, *Proc. Natl. Acad. Sci. U.S.A. 100*, 3784−3789.
56. van Leusen, D., and van Leusen, A. (1980) A simple synthesis of cyclobutanone, *Synthesis 4*, 325−326.
57. Bloomquist, A. T., Passer, M., and Schollenberger, C. S. (1957) Thermal Condensation of Formaldehyde with Acyclic Olefins, *J. Am. Chem. Soc. 79*, 4972−4976.
58. Marvel, C. S., Myers, R. L., and Saunders, J. H. (1948) The Preparation of 2-Alkylbutadienes, *J. Am. Chem. Soc. 70*, 1694−1699.
59. Xia, B., Pikus, J. D., Xia, W., McClay, K., Steffan, R. J., Chae, Y. K., Westler, W. M., Markley, J. L., and Fox, B. G. (1999) Detection and classification of hyperfine-shifted ^{1}H, ^{2}H, and ^{15}N resonances of the Rieske ferredoxin component from toluene 4-monooxygenase, *Biochemistry 38*, 727−739.
60. Studts, J. M., Mitchell, K. H., Pikus, J. D., McClay, K., Steffan, R. J., and Fox, B. G. (2000) Optimized expression and purification of toluene 4-monooxygenase hydroxylase, *Protein Expression Purif. 20*, 58−65.
61. Hemmi, H., Studts, J. M., Chae, Y. K., Song, J., Markley, J. L., and Fox, B. G. (2001) Solution structure of the toluene 4-monooxygenase effector protein (T4moD), *Biochemistry 40*, 3512−3524.
62. Ruzicka, F., Huang, D.-S., Donnelly, M. I., and Frey, P. A. (1990) Methane monooxygenase catalyzed oxidation of 1,1-dimethylcyclopropane. Evidence for radical and carbocationic intermediates, *Biochemistry 29*, 1696−1700.
63. Lyle, K. S., Ai, J., Moenne-Loccoz, P., Sanders-Loehr, J., Loehr, T. M., and Fox, B. G. (2000) Resonance Raman studies of the stoichiometric catalytic turnover of a substrate-stearoyl-acyl carrier protein Δ^9 desaturase complex, *Biochemistry 39*, 10507−10513.
64. Newcomb, M., Shen, R., Lu, Y., Coon, M. J., Hollenberg, P. F., Kopp, D. A., and Lippard, S. J. (2002) Evaluation of norcarane as a probe for radicals in cytochrome P450- and soluble methane monooxygenase-catalyzed hydroxylation reactions, *J. Am. Chem. Soc. 124*, 6879−6886.
65. Canada, K. A., Iwashita, S., Shim, H., and Wood, T. K. (2002) Directed evolution of toluene ortho-monooxygenase for enhanced 1-naphthol synthesis and chlorinated ethene degradation, *J. Bacteriol. 184*, 344−349.
66. Rui, L., Kwon, Y. K., Fishman, A., Reardon, K. F., and Wood, T. K. (2004) Saturation Mutagenesis of Toluene *ortho*-Monooxygenase of *Burkholderia cepacia* G4 for Enhanced 1-Naphthol Synthesis and Chloroform Degradation, *Appl. Environ. Microbiol. 70*, 3246−3252.
67. Vardar, G., and Wood, T. K. (2004) Protein Engineering of Toluene-*o*-Xylene Monooxygenase from Pseudomonas stutzeri OX1 for Synthesizing 4-Methylresorcinol, Methylhydroquinone, and Pyrogallol, *Appl. Environ. Microbiol 70*, 3253−3262.
68. Åberg, A., Ormö, M., Nordlund, P., and Sjöberg, B.-M. (1993) Autocatalytic generation of dopa in the engineered protein R2 F208Y from *Escherichia coli* ribonucleotide reductase and crystal structure of the dopa-208 protein, *Biochemistry 32*, 9845−9850.
69. Logan, D. T., deMaré, F., Persson, B. O., Slaby, A., Sjöberg, B.-M., and Nordlund, P. (1998) Crystal structure of two self-hydroxylating ribonucleotide reductase protein R2 mutants: structural basis for the oxygen-insertion step catalyzed by the diiron proteins, *Biochemistry 37*, 10798−10807.
70. Ormö, M., deMaré, F., Regnström, K., Åberg, A., Sahlin, M., Ling, J., Loehr, T. M., Sanders-Loehr, J., and Sjöberg, B.-M. (1992) Engineering of the iron site in ribonucleotide reductase to a self-hydroxylating monooxygenase, *J. Biol. Chem. 267*, 8711−8714.
71. Ling, J., Sahlin, M., Sjöberg, B.-M., Loehr, T. M., and Sanders-Loehr, J. (1994) Dioxygen is the source of the oxo bridge in ribonucleotide reductase, *J. Biol. Chem. 269*, 5596−5601.
72. Baldwin, J., Voegtli, W. C., Khidekel, N., Moënne-Loccoz, P., Krebs, C., Pereira, A. S., Ley, B. A., Huynh, B. H., Loehr, T. M., Riggs-Gelasco, P. J., Rosenzweig, A. C., and Bollinger, J. M., Jr. (2001) Rational reprogramming of the R2 subunit of *Escherichia coli* ribonucleotide reductase into a self-hydroxylating monooxygenase, *J. Am. Chem. Soc. 123*, 7017−7030.
73. Voegtli, W. C., Khidekel, N., Baldwin, J., Ley, B. A., Bollinger, J. M., Jr., and Rosenzweig, A. C. (2000) Crystal structure of the ribonucleotide reductase R2 mutant that accumulates a μ-1,2-peroxodiiron(III) intermediate during oxygen activation, *J. Am. Chem. Soc. 122*, 3255−3261.
74. White, R. D., and Fox, B. G. (2003) Chain cleavage and sulfoxidation of thiastearoyl-ACP upon reaction with stearoyl-ACP desaturase, *Biochemistry 42*, 7828−7835.
75. Rogge, C. E., and Fox, B. G. (2002) Desaturation, chain scission, and register-shift of oxygen-substituted fatty acids during reaction with stearoyl-ACP desaturase, *Biochemistry 41*, 10141−10148.
76. Fox, B. G., Lyle, K. S., and Rogge, C. E. (2004) Reactions of the diiron enzyme stearoyl-ACP desaturase, *Acc. Chem. Res. 37*, 421−429.
77. Nordlund, P., and Eklund, H. (1993) Structure and function of the *Escherichia coli* ribonucleotide reductase protein R2, *J. Mol. Biol. 232*, 123−164.
78. Lee, S.-K., and Lipscomb, J. D. (1999) Oxygen activation catalyzed by methane monooxygenase hydroxylase component: Proton delivery during the O−O bond cleavage steps, *Biochemistry 38*, 4423−4432.

BI040033H